

Modifications of the Trefftz Method for Estimating the Contribution of the Hall Effect on Magnetotelluric Sounding

V.V. Plotkin^{a, ✉}, V.S. Mogilatov^{a,b}, V.V. Potapov^a

^a Trofimuk Institute of Petroleum Geology and Geophysics, Siberian Branch of the Russian Academy of Science,
pr. Akademika Koptyuga 3, Novosibirsk, 630090, Russia

^b Novosibirsk State University, ul. Pirogova 2, Novosibirsk, 630090, Russia

Received 6 October 2017; received in revised form 2 February 2018; accepted 1 March 2018

Abstract—Possible manifestations of the Hall effect in the Earth's magnetic field during magnetotelluric sounding are considered. Numerical calculations of the magnitude the effect for a three-dimensional heterogeneous earth, using modifications of the Trefftz method suitable for accounting for anisotropy are made for. Versions of the measurement that allow easy detection of manifestations of the Hall effect are analyzed.

Keywords: magnetotelluric sounding of a three-dimensional heterogeneous earth, Hall effect, Trefftz method, electrical conductivity

INTRODUCTION

Many minerals are semiconductors according to the physical mechanism of electrical conduction in them (Shuey, 1975). Host rocks above petroleum deposits penetrated by hydrocarbon fluid flow are also a semiconducting medium (Gololobov and Malevich, 2005). One of the main experimental methods for determining the electrical conductivity parameters of semiconducting minerals (density and mobility of current carriers) is based on the Hall effect. Therefore, due to the presence of the Earth's magnetic field during electromagnetic sounding, it is quite possible to expect manifestations of this effect for minerals occurring in rocks under natural conditions. Interest in this phenomenon first arose in connection with the results of controlled-source electromagnetic sounding in areas of hydrocarbon accumulations (Mogilatov, 2013).

A difficulty is that the electrical conductivity of semiconductors varies widely depending on the presence of lattice impurities and heterogeneities and temperature and acoustic oscillations (Bush, 1952). The experimental results of laboratory measurements reported in the literature depend on the method of sample preparation. All these factors greatly complicate the preliminary evaluation of the magnitude of the presumed effect.

An important issue for the detection of the Hall effect under natural conditions is the magnitude of the Hall conductivity of the medium. In laboratory experiments with samples, it is common to measure the conductivity σ and the

Hall constant R_H of semiconductors. Simultaneous measurements of conductivity and the Hall effect are required to elucidate the conduction mechanism. They allow a determination of the Hall mobility μ_e , the current carrier density, and the type of conductivity (electronic, hole or mixed) and a rough estimation of the Hall conductivity $\sigma_H \approx \sigma \mu_e B$ (B is the geomagnetic field induction). We note that the latter relation is suitable only for laboratory experiments where the results of simultaneous measurements of σ and R_H are obtained and the measured semiconductor is known. Since the conductivity of semiconductors depends on the type of current carriers, the Hall mobility μ_e may differ from the ordinary drift mobility used in practice to evaluate the electrical conductivity of rocks σ . An arbitrary rock should be considered only as some new sample for which simultaneous measurements of conductivity and the Hall effect are also required. Formal application of the relation $\sigma_H \approx \sigma \mu_e B$ to an earth with specified electrical conductivity without simultaneous measurements of σ and σ_H may lead to incorrect estimates of the current carrier mobility μ_e and the dimensionless parameter $\mu_e B$ and, ultimately, to manifestations of the Hall effect in order of magnitude. Therefore, the question arises as to how to carry out simultaneous measurements of σ and σ_H in practice and which methods are preferred for this.

It is also important that in the absence of direct experimental measurements of the indicated earth parameters, it is only possible to speak of particular assumptions on the physical nature of mobility. In this regard, we can recall the flow of a viscous conductive fluid in a magnetic field (Hartmann flow). There is some analogy with the movement of fluids in a porous medium. It is difficult to say what the characteristics of this process are. For the time being, it is

✉ Corresponding author.

E-mail adress: PlotkinVV@ipgg.sbras.ru (V.V. Plotkin)

better to speak of the effective mobility of current carriers in the earth. Estimates of its magnitude will be made possible by simultaneous experimental field measurements of σ and σ_H .

Analysis of the results of laboratory experimental measurements of the conductivity of various ore minerals (Parkhomenko, 1967; Shuey, 1975) shows that in some cases, it is possible to expect values $\sigma_H \leq 0.001$ S/m. For example, for galena samples with an average conductivity of ~ 1000 S/m and mobilities $\mu_e \sim 200$ cm²/V·s and $B \sim 5 \times 10^{-5}$ T, the Hall conductivity $\sigma_H = 0.001$ S/m. Pyrite has somewhat lower Hall conductivity as many published values of the electron mobility are in the range 10–50 cm²/V·s at the same average conductivity of the samples. Pyrite determines the electrical conductivity of sulfur pyrite, whose value varies widely depending on the amount of pyrite. The wide range of electrical conductivity of rocks (about twenty orders of magnitude) is due to the properties and composition of the various minerals contained in them. The same is true for the possible values of the Hall conductivity of rocks. Therefore, the use of any of its reliable values will be possible only after experimental measurements of σ_H under natural conditions.

To properly plan experimental work and select appropriate electromagnetic methods, it is necessary to obtain numerical estimates of the contribution of the Hall effect to the measurement results. This will allow a priori determination of Hall conductivity values that can be detected by modern electromagnetic methods under natural conditions. Methods for the experimental determination of σ_H are also needed.

A method for calculating the contribution of the Hall effect in magnetotelluric sounding (MTS) of a horizontally layered earth was proposed in (Plotkin, 2017). It involves determining mode impedances when calculating the response to the excitation of the earth by waves with different polarization. Due to the Hall effect, the response of the earth may be different in the cases where the earth is excited by only one of the normal waves occurring in the anisotropic case. By choosing experimental sessions with different directions of rotation of the electric or magnetic field vectors, it is possible to determine the impedance tensor separately for these waves. It has also been shown how to convert from the total impedance tensor to mode impedances without separating the sessions according to different modes.

In practice, the situation is complicated by the presence of lateral conductivity heterogeneities. In this study, numerical estimates of the contribution of the Hall effect were obtained for a three-dimensional heterogeneous earth using the Trefftz method to calculate the magnetotelluric field (Egorov, 2011).

TREFFTZ METHOD FOR A MEDIUM IN THE GEOMAGNETIC FIELD

We will consider the possible influence of the Earth's magnetic field on MTS results, taking into account the Hall conductivity of the medium σ_H . We use Cartesian coordi-

nates with the OX axis pointing to the north magnetic pole, the OZ axis pointing downward into the medium, and the OY axis perpendicular to the plane of the magnetic meridian. In this coordinate system, the conductivity tensor $\hat{\sigma}$ has the form

$$\hat{\sigma} = \begin{pmatrix} \sigma & -\sigma_H \cos(\vartheta) & 0 \\ \sigma_H \cos(\vartheta) & \sigma & -\sigma_H \sin(\vartheta) \\ 0 & \sigma_H \sin(\vartheta) & \sigma \end{pmatrix}, \quad (1)$$

where σ is the ordinary electrical conductivity of the medium and ϑ is the angle between the magnetic field vector and the vertical direction. The tensor reciprocal to (1) is given by

$$\hat{\sigma}^{-1} = \frac{1}{\sigma(1+\xi^2)} \begin{pmatrix} 1+\xi^2 \sin^2 \vartheta & \xi \cos \vartheta & \xi^2 \sin \vartheta \cos \vartheta \\ -\xi \cos \vartheta & 1 & \xi \sin \vartheta \\ \xi^2 \sin \vartheta \cos \vartheta & -\xi \sin \vartheta & 1+\xi^2 \cos^2 \vartheta \end{pmatrix}, \quad (2)$$

where $\xi = \sigma_H/\sigma$. Depending on the value of ξ , there may be different versions of the application of the Trefftz method to the study of manifestations of the Hall effect in a three-dimensional heterogeneous anisotropic earth.

As is known, in the Trefftz method, the computational domain is represented by a set of parallelepiped finite elements in which the medium is homogeneous. For the isotropic case, the solutions of the Maxwell equations in the form of transverse counter-propagating waves moving along each of the coordinate axes are used in each parallelepiped. With consideration of the polarization, there are 12 such waves, whose unknown amplitudes are found from the matching conditions on all faces of the above-mentioned parallelepipeds and from the boundary conditions.

In an anisotropic medium, the wave polarization degeneracy is removed. The waves called normal in optics propagate along the coordinate axes at different speeds depending on polarization. Let us consider how these waves can be used to numerically solve the Maxwell equations using the Trefftz method.

Modification of the Trefftz method with normal waves. We consider a horizontally layered earth—a normal section $\sigma_0(z)$ with parameters $\sigma_n, h_n, n = 1, \dots, N, h_N \rightarrow \infty$. Let $\mathbf{E}_0(z)$ be the normal field that occurs in this medium during magnetotelluric sounding. Suppose further that the Earth's constant magnetic field in this medium gives rise to the Hall conductivity, and the electrical conductivity of the medium becomes the tensor quantity (1).

To study manifestation of the Hall effect in the three-dimensional heterogeneous medium, we assume that in (1) and (2), all quantities (except for ϑ) depend not only on z but also on the horizontal coordinates. In this situation, it is more convenient to perform calculations for the anomalous field \mathbf{E} that occurs due to the anisotropy and 3D heterogeneity of the medium, in addition to the normal field $\mathbf{E}_0(z)$. Considering that

$$\Delta \mathbf{E}_0 - k_0^2(z) \mathbf{E}_0 = 0, \quad k_0^2 = i\omega \mu \sigma_0(z), \quad (3)$$

for the anomalous field \mathbf{E} , we obtain an equation with the right side

$$\Delta \mathbf{E} - \text{grad div } \mathbf{E} - i\omega\mu \hat{\sigma} \mathbf{E} = i\omega\mu(\hat{\sigma} - \sigma_0 \hat{I}) \mathbf{E}_0(z), \quad (4)$$

where \hat{I} is the unit tensor. Next, we will need the particular solution (4) associated with the presence of the right side. Neglecting the dependence of the field $\mathbf{E}_0(z)$ on z inside the parallelepipeds and taking into account the homogeneity of the medium in them, we can write this particular solution in the form

$$\mathbf{E}_d = (\sigma_0 \hat{\sigma}^{-1} - \hat{I}) \mathbf{E}_0. \quad (5)$$

In an anisotropic medium, we need to use the solutions of equation (4). They can be found by sequentially assuming that the field depends on only one coordinate. The combination of these solutions contains waves with 12 unknown amplitudes, and for any of the parallelepipeds, it has the form

$$\begin{aligned} E_x = & -2i \cos \vartheta \left[a_1 e^{k_{1z}(z-z_l)} + a_2 e^{-k_{1z}(z-z_l)} \right. \\ & \left. + a_3 e^{k_{2z}(z-z_l)} + a_4 e^{-k_{2z}(z-z_l)} \right] \\ & - \cos \vartheta \left[a_5 e^{k_{1y}(y-y_n)} + a_6 e^{-k_{1y}(y-y_n)} \right] \\ & + \sin \vartheta \left[a_7 e^{k_{2y}(y-y_n)} + a_8 e^{-k_{2y}(y-y_n)} \right] \\ & - \xi \sin \vartheta \cos \vartheta \left[a_9 e^{k_{1x}(x-x_m)} + a_{10} e^{-k_{1x}(x-x_m)} \right. \\ & \left. + a_{11} e^{k_{2x}(x-x_m)} + a_{12} e^{-k_{2x}(x-x_m)} \right] \\ & + \frac{\eta - 1 - \xi^2 (1 - \eta \sin^2 \vartheta)}{1 + \xi^2} E_{0x} + \frac{\eta \xi \cos \vartheta}{1 + \xi^2} E_{0y}, \\ E_y = & Q_+ \left[a_1 e^{k_{1z}(z-z_l)} + a_2 e^{-k_{1z}(z-z_l)} \right] \\ & + Q_- \left[a_3 e^{k_{2z}(z-z_l)} + a_4 e^{-k_{2z}(z-z_l)} \right] \\ & - \sin \vartheta \left[a_9 e^{k_{1x}(x-x_m)} + a_{10} e^{-k_{1x}(x-x_m)} + a_{11} e^{k_{2x}(x-x_m)} + a_{12} e^{-k_{2x}(x-x_m)} \right] \\ & + \xi \left[a_5 e^{k_{1y}(y-y_n)} + a_6 e^{-k_{1y}(y-y_n)} \right] - \frac{\eta \xi \cos \vartheta}{1 + \xi^2} E_{0x} + \frac{\eta - 1 - \xi^2}{1 + \xi^2} E_{0y}, \\ E_z = & -\xi \sin \vartheta \left(Q_+ \left[a_1 e^{k_{1z}(z-z_l)} + a_2 e^{-k_{1z}(z-z_l)} \right] \right. \\ & \left. + Q_- \left[a_3 e^{k_{2z}(z-z_l)} + a_4 e^{-k_{2z}(z-z_l)} \right] \right) \\ & + \sin \vartheta \left[a_5 e^{k_{1y}(y-y_n)} + a_6 e^{-k_{1y}(y-y_n)} \right] \\ & + \cos \vartheta \left[a_7 e^{k_{2y}(y-y_n)} + a_8 e^{-k_{2y}(y-y_n)} \right] \\ & + P_+ \left[a_9 e^{k_{1x}(x-x_m)} + a_{10} e^{-k_{1x}(x-x_m)} \right] \\ & + P_- \left[a_{11} e^{k_{2x}(x-x_m)} + a_{12} e^{-k_{2x}(x-x_m)} \right] \end{aligned}$$

$$+ \frac{\eta \xi^2 \sin \vartheta \cos \vartheta}{1 + \xi^2} E_{0x} - \frac{\eta \xi \sin \vartheta}{1 + \xi^2} E_{0y}, \quad (6)$$

$$H_x = \frac{1}{i\omega\mu} \left\{ k_{1z} Q_+ \left[a_1 e^{k_{1z}(z-z_l)} - a_2 e^{-k_{1z}(z-z_l)} \right] \right.$$

$$+ k_{2z} Q_- \left[a_3 e^{k_{2z}(z-z_l)} - a_4 e^{-k_{2z}(z-z_l)} \right]$$

$$- k_{1y} \sin \vartheta \left[a_5 e^{k_{1y}(y-y_n)} - a_6 e^{-k_{1y}(y-y_n)} \right]$$

$$- k_{2y} \cos \vartheta \left[a_7 e^{k_{2y}(y-y_n)} - a_8 e^{-k_{2y}(y-y_n)} \right] \left. \right\}$$

$$+ \frac{\eta \xi \cos \vartheta}{1 + \xi^2} H_{0y} + \frac{\eta - 1 - \xi^2}{1 + \xi^2} H_{0x},$$

$$H_y = \frac{1}{i\omega\mu} \left\{ 2ik_{1z} \cos \vartheta \left[a_1 e^{k_{1z}(z-z_l)} - a_2 e^{-k_{1z}(z-z_l)} \right] \right.$$

$$+ 2ik_{2z} \cos \vartheta \left[a_3 e^{k_{2z}(z-z_l)} - a_4 e^{-k_{2z}(z-z_l)} \right]$$

$$+ k_{1x} P_+ \left[a_9 e^{k_{1x}(x-x_m)} - a_{10} e^{-k_{1x}(x-x_m)} \right]$$

$$+ k_{2x} P_- \left[a_{11} e^{k_{2x}(x-x_m)} - a_{12} e^{-k_{2x}(x-x_m)} \right]$$

$$- \frac{\eta \xi \cos \vartheta}{1 + \xi^2} H_{0x} + \frac{\eta - 1 - \xi^2 (1 - \eta \sin^2 \vartheta)}{1 + \xi^2} H_{0y},$$

$$H_z = \frac{1}{i\omega\mu} \left\{ -k_{1y} \cos \vartheta \left[a_5 e^{k_{1y}(y-y_n)} - a_6 e^{-k_{1y}(y-y_n)} \right] \right.$$

$$+ k_{2y} \sin \vartheta \left[a_7 e^{k_{2y}(y-y_n)} - a_8 e^{-k_{2y}(y-y_n)} \right]$$

$$+ k_{1x} \sin \vartheta \left[a_9 e^{k_{1x}(x-x_m)} - a_{10} e^{-k_{1x}(x-x_m)} \right]$$

$$+ k_{2x} \sin \vartheta \left[a_{11} e^{k_{2x}(x-x_m)} - a_{12} e^{-k_{2x}(x-x_m)} \right] \left. \right\},$$

where

$$k_{1x, 2x}^2 = k_0^2 \left[1 + \frac{1}{2} \xi^2 \cos^2(\vartheta) \pm i \sqrt{\xi^2 \sin^2(\vartheta) - \frac{1}{4} \xi^4 \cos^4(\vartheta)} \right],$$

$$k_{1z, 2z}^2 = k_0^2 \left[1 + \frac{1}{2} \xi^2 \sin^2(\vartheta) \pm i \sqrt{\xi^2 \cos^2(\vartheta) - \frac{1}{4} \xi^4 \sin^4(\vartheta)} \right],$$

$$k_{1y}^2 = k_0^2 (1 + \xi^2), \quad k_{2y}^2 = k_0^2,$$

$$P_{\pm} = -\frac{\xi}{2} \cos^2 \vartheta \pm \sqrt{\frac{\xi^2}{4} \cos^4 \vartheta - \sin^2 \vartheta},$$

$$Q_{\pm} = i \xi \sin^2 \vartheta \pm \sqrt{4 \cos^2 \vartheta - \xi^2 \sin^4 \vartheta}, \quad \eta = \sigma_0 / \sigma.$$

As can be seen, the general solution for the anomalous field (6) consists of the solution of the homogeneous equation (4) and the particular solution which appears due to the

presence of the right-hand side in (4). For the electric field, it is obtained from (5), and for the magnetic field, it is found using the equation $\text{rot}\mathbf{E}_0 = -i\omega\mu \mathbf{H}_0$ and taking into account the dependence of the field $\mathbf{E}_0(z)$ on only one coordinate z . The particular solution determines the contribution to the anomalous field from the Hall conductivity σ_H (the parameter ξ) and the 3D-deviations of the electrical conductivity σ from the normal section $\sigma_0(z)$ (the parameter η). Expressions (6) take into account the polarization of the fields of the anisotropic components (the relation between the components of the fields). Changes in the fields of anisotropic components along the corresponding coordinate axes relative to the centers of the parallelepipeds $x_m, y_n,$ and z_l are characterized by the wavenumbers $k_{1x,2x}, k_{1y,2y},$ and $k_{1z,2z}$. Calculations of the field $\mathbf{E}_0(z)$ as a function of the depth are performed using the method described in (Aleksandrov, 2001; Plotkin, 2017).

To determine the unknown amplitudes a_1, \dots, a_{12} (6) in all parallelepipeds, it is necessary to solve the system of algebraic equations obtained from the boundary conditions and the matching conditions of solutions (6) between adjacent parallelepipeds. For this, the continuity conditions for the tangential components of the electric and magnetic fields are specified at the central points of all the inner faces of the adjacent parallelepipeds constituting the computational domain.

On the outer surface of the computational domain, we specify external boundary conditions (BC) that correspond to the decay of the anomalous field outside this region. The BCs at the upper and lower boundaries of the computational domain can be specified using two-dimensional Fourier transforms of the field along horizontal coordinates (Plotkin and Gubin, 2015).

There may also be another version of BCs: in those parallelepipeds one face of which is adjacent to the outer boundary of the computational domain, the amplitudes of all waves coming from the outside, i.e., increasing toward the outer boundary of the region, are set equal to zero. This implies the absence of anomalous field sources outside the computational domain. In addition to the parallelepipeds at the lateral boundaries (in which the earth model is assumed to correspond to the normal section), the computational domain also includes two additional homogeneous layers: the upper atmospheric layer and the lower underlying layer. In all the mentioned boundary parallelepipeds of the computational domain, it is assumed that $\eta = 1$ and $\xi = 0$. These boundary conditions simplify the matrix of the system of algebraic equations for determining the unknown wave amplitudes in (6). Naturally, the number of equations taking into account all the matching conditions and external BCs is equal to the total number of unknown amplitudes.

Experience has shown that the modification of the Trefftz method described above works well for fairly large values of ξ as long as the differences between the characteristics of the normal waves propagating in the same direction are significant. Depending on the earth model, the matrix of the

system of equations for determining the amplitudes a_1, \dots, a_{12} in (6) may turn out to be close to singular as ξ decreases. Therefore, for a small value of ξ , it is preferred to use a different approach.

Modification of the Trefftz method for small ξ . In the previous case, the entire field occurring in addition $\mathbf{E}_0(z)$ —the normal field in a horizontally layered earth—was considered anomalous. For low Hall conductivity and small differences between the normal waves, the use of the Trefftz method is more reliable only when using the solutions for the isotropic case in the parallelepipeds. For this purpose, we now assume that the perturbations of the fields \mathbf{E}_d and \mathbf{H}_d due only to the Hall effect are anomalous. Let $\mathbf{E}_0(x, y, z)$ and $\mathbf{H}_0(x, y, z)$ be numerical solutions for an isotropic three-dimensionally heterogeneous earth with electrical conductivity $\sigma(x, y, z)$. Then the Maxwell equations the anomalous fields can be written as

$$\begin{aligned} \text{rot}\hat{\sigma}^{-1}\text{rot}\mathbf{H} &= -i\omega\mu\mathbf{H}, \quad \mathbf{H} = \mathbf{H}_d + \mathbf{H}_0, \\ \text{rot}\sigma^{-1}\text{rot}\mathbf{H}_0 &= -i\omega\mu\mathbf{H}_0, \\ \text{rot}\hat{\sigma}^{-1}\text{rot}\mathbf{H}_d + i\omega\mu\mathbf{H}_d &= \text{rot}\left(\frac{\hat{I}}{\sigma} - \hat{\sigma}^{-1}\right)\text{rot}\mathbf{H}_0 = \\ \text{rot}\left(\hat{I} - \sigma\hat{\sigma}^{-1}\right)\mathbf{E}_0, \end{aligned} \tag{7a}$$

$$\begin{aligned} \text{rotrot}\mathbf{E} &= -i\omega\mu\hat{\sigma}\mathbf{E}, \quad \mathbf{E} = \mathbf{E}_d + \mathbf{E}_0, \quad \text{rotrot}\mathbf{E}_0 = -i\omega\mu\sigma\mathbf{E}_0, \\ \text{rotrot}\mathbf{E}_d + i\omega\mu\hat{\sigma}\mathbf{E}_d &= i\omega\mu(\sigma - \hat{\sigma})\mathbf{E}_0. \end{aligned} \tag{7b}$$

Given the smallness $\xi = \sigma_H/\sigma \ll 1$, the solutions for the isotropic case can be used on the left sides of the equations for \mathbf{E}_d and \mathbf{H}_d as the main solutions in the parallelepipeds when using the Trefftz method. In this case, the contribution of the Hall conductivity is determined by the right-hand sides of equations (7) with the help of approximate particular solutions added to the main ones in the parallelepipeds for the isotropic case:

$$\begin{aligned} \mathbf{H}_p &= -\frac{1}{i\omega\mu} \text{rot}\left(\sigma\hat{\sigma}^{-1} - \hat{I}\right)\mathbf{E}_0, \\ \mathbf{H}_p &= -\frac{\xi}{i\omega\mu} \left(\sin\vartheta \frac{\partial}{\partial x} + \cos\vartheta \frac{\partial}{\partial z}\right)\mathbf{E}_0, \\ \mathbf{E}_p &= \left(\sigma\hat{\sigma}^{-1} - \hat{I}\right)\mathbf{E}_0, \quad \text{rot}\mathbf{E}_0 = -i\omega\mu\mathbf{H}_0, \end{aligned} \tag{8}$$

$$\sigma\hat{\sigma}^{-1} - \hat{I} \approx \begin{pmatrix} 0 & \xi \cos\vartheta & 0 \\ -\xi \cos\vartheta & 0 & \xi \sin\vartheta \\ 0 & -\xi \sin\vartheta & 0 \end{pmatrix}, \tag{9}$$

$$\mathbf{H}_p = \left(\sigma\hat{\sigma}^{-1} - \hat{I}\right)\mathbf{H}_0 - \frac{\xi}{i\omega\mu} \nabla(\mathbf{n}\mathbf{E}_0), \quad \mathbf{n} = (\sin\vartheta, 0, \cos\vartheta). \tag{10}$$

The particular solutions for \mathbf{H}_p and \mathbf{E}_p in (8) are obtained from (7) neglecting the dependence of the field \mathbf{E}_0 on the coordinates inside the parallelepipeds and taking into account the homogeneity of the medium in them. The tensor in (9) is written up to terms linear in ξ . Experience has shown that the use of spatial derivatives of \mathbf{E}_0 in (8) is not possible because of their unsatisfactory approximation in numerical calculations by the Trefftz method. However, the solution for \mathbf{H}_p can be reduced to the form (10). As can be seen from (10), the solution without the above derivatives is valid if we neglect the component of \mathbf{E}_0 longitudinal along the Earth's magnetic field. For MTS and approximate estimation of the contribution of σ_H , this is quite acceptable. Then the particular solutions \mathbf{E}_p and \mathbf{H}_p added to the main solutions in the parallelepipeds for the isotropic case have a very simple form and are calculated in the same way using the tensor (9) (it is interesting to compare them with those given in (6) for $\eta = 1$ with consideration of only terms linear in ξ).

As regards the matching and boundary conditions, the above remains true in this version of the application of the Trefftz method. Note that in the latter version, it was more convenient to implement the software using boundary conditions based on two-dimensional Fourier transforms (Plotkin and Gubin, 2015).

RESULTS OF NUMERICAL CALCULATIONS AND THEIR DISCUSSION

To verify the performance of software based on the Trefftz method, we first performed numerical calculations for the horizontally layered earth model (upper layers of the Earth's crust) taken from (Plotkin, 2017). It uses a matrix numerical method to solve Maxwell's equations as a system of first-order equations (Aleksandrov 2001). The horizontally layered model is represented by four layers with top-to-bottom thicknesses of 0.7, 5, 2, and 9 km and resistivities of 100, 1000, 300 and 100 Ohm·m, respectively, and an underlying medium with a resistivity of 20 Ohm·m. The Hall conductivity was set equal to 1/1000 S/m, and the angle between the magnetic field and the vertical direction $\vartheta = 25^\circ$.

The procedure of numerical calculations described in (Aleksandrov, 2001) yields the standard impedance tensor independent of the directions of rotation of the field vectors. To take this into account, it has been proposed (Plotkin, 2017) to use the mode impedances $Z_{xy}^{m_{1,2}}$, $Z_{xx}^{m_{1,2}}$, $Z_{yx}^{m_{1,2}}$, and $Z_{yy}^{m_{1,2}}$:

$$\begin{aligned} E_{x_{1,2}} &= (Z_{xx}g_{1,2} + Z_{xy})H_{y_{1,2}}, & Z_{xy}^{m_{1,2}} &= E_{x_{1,2}} / H_{y_{1,2}}, \\ E_{x_{1,2}} &= (Z_{xx} + Z_{xy} / g_{1,2})H_{x_{1,2}}, & Z_{xx}^{m_{1,2}} &= E_{x_{1,2}} / H_{x_{1,2}}, \\ E_{y_{1,2}} &= (Z_{yx} + Z_{yy} / g_{1,2})H_{x_{1,2}}, & Z_{yx}^{m_{1,2}} &= E_{y_{1,2}} / H_{x_{1,2}}, \\ E_{y_{1,2}} &= (Z_{yx}g_{1,2} + Z_{yy})H_{y_{1,2}}, & Z_{yy}^{m_{1,2}} &= E_{y_{1,2}} / H_{y_{1,2}}, \end{aligned} \quad (11)$$

where $g_{1,2}$ are the polarization coefficients of the normal waves 1 and 2. As can be seen from (11), to calculate the mode impedances for the components of the standard impedance tensor, it is necessary to know the coefficients $g_{1,2}$. Generally speaking, for a horizontally layered earth, they vary from layer to layer. However, it can be shown and confirmed by calculations that in mid-latitudes and for a weak effect, when $\sigma_H \ll \sigma_n$, these coefficients are close to the values of $g_{1,2} = \pm i$ used in the calculations. To display the results, all the impedances in (11) were converted by the usual formulas into apparent resistivity curves and phase curves.

In the calculations using the Trefftz method, the test site had dimensions of 15×15 km and was divided into five parallelepipeds along the OX and OY axes (the dimensions of the parallelepipeds in the horizontal section were 3×3 km; a total of 25 parallelepipeds in each layer). In the version of the Trefftz method with normal waves, we added homogeneous layers: an atmospheric layer 1 m thick at the top and an underlying layer 1 km thick with a resistivity of 20 Ohm·m at the bottom. In this case, the total number of parallelepipeds increased to 150 (in the version for small ξ to 100).

The calculation results are shown in Fig. 1. One can see good qualitative agreement between the dependences of the curves on the time period obtained by different numerical methods. At the same time, the approximate nature of the calculations allows only rough estimation of the magnitude of the effect. For more accurate calculations using the Trefftz method, it is necessary to increase the number of parallelepipeds in the computational domain, which will require a corresponding increase in computational costs. However, some conclusions can be drawn now. Comparison of the standard curves and the mode curves (only the curves of ρ_{xy} for both normal waves are given since the curves of ρ_{yx} differ from them only slightly) shows that the latter are much more significantly affected by the Hall effect. We note that the effect will remain noticeable even for smaller (by one or two orders of magnitude) values of the Hall conductivity.

Another earth model was also considered to evaluate the contribution of deeper crustal layers and lateral heterogeneities. Stable results for this model were obtained in calculations using the version of the Trefftz method for small ξ . In this case, the earth model was represented by four layers with top-to-bottom thicknesses of 0.01, 15, 10, and 45 km and resistivities of 1, 1000, 10, and 100 Ohm·m, respectively, and an underlying medium with a resistivity of 10 Ohm·m. The upper layer was used to simulate the distortions of MTS curves caused by near-surface lateral heterogeneities. For this purpose, the resistivity in the central parallelepiped of the upper layer was set equal to 0.2 Ohm·m. The model also included a crustal conductive layer 10 km thick with a roof at a depth of ~ 15 km with a resistivity of 10 Ohm·m and a mantle a conductive layer with a roof at a depth of ~ 70 km with a resistivity of 10 Ohm·m. The Hall conductivity was set equal to 1/2000 S/m and the angle be-

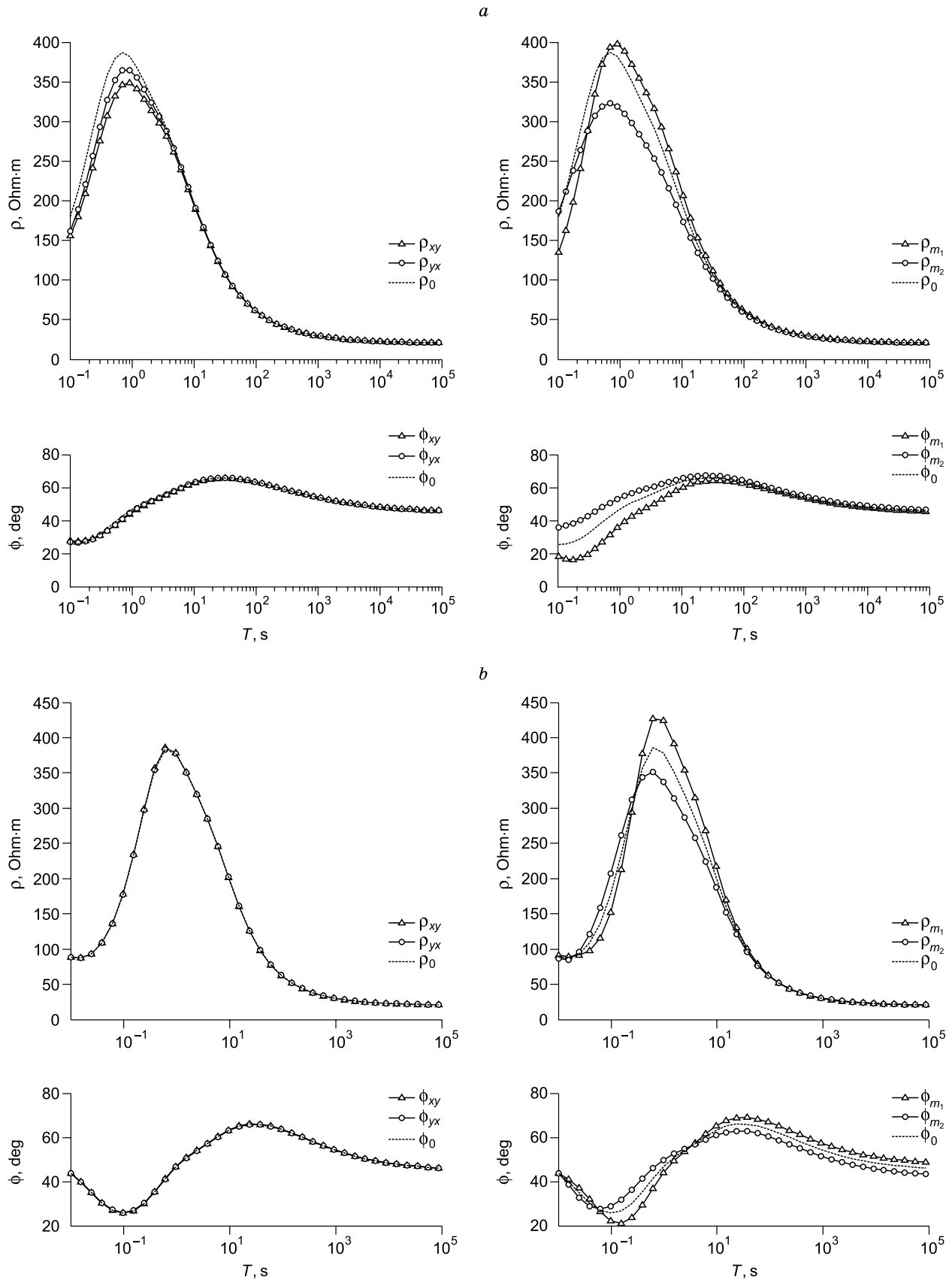


Fig. 1. MTS curves (on the left are the standard curves, on the right are the mode curves, and the dotted lines show the curves for $\sigma_H = 0$). The calculations were performed using the method of (Plotkin, 2017) (a) and the Trefftz method for small ξ (b) and with normal waves (c).

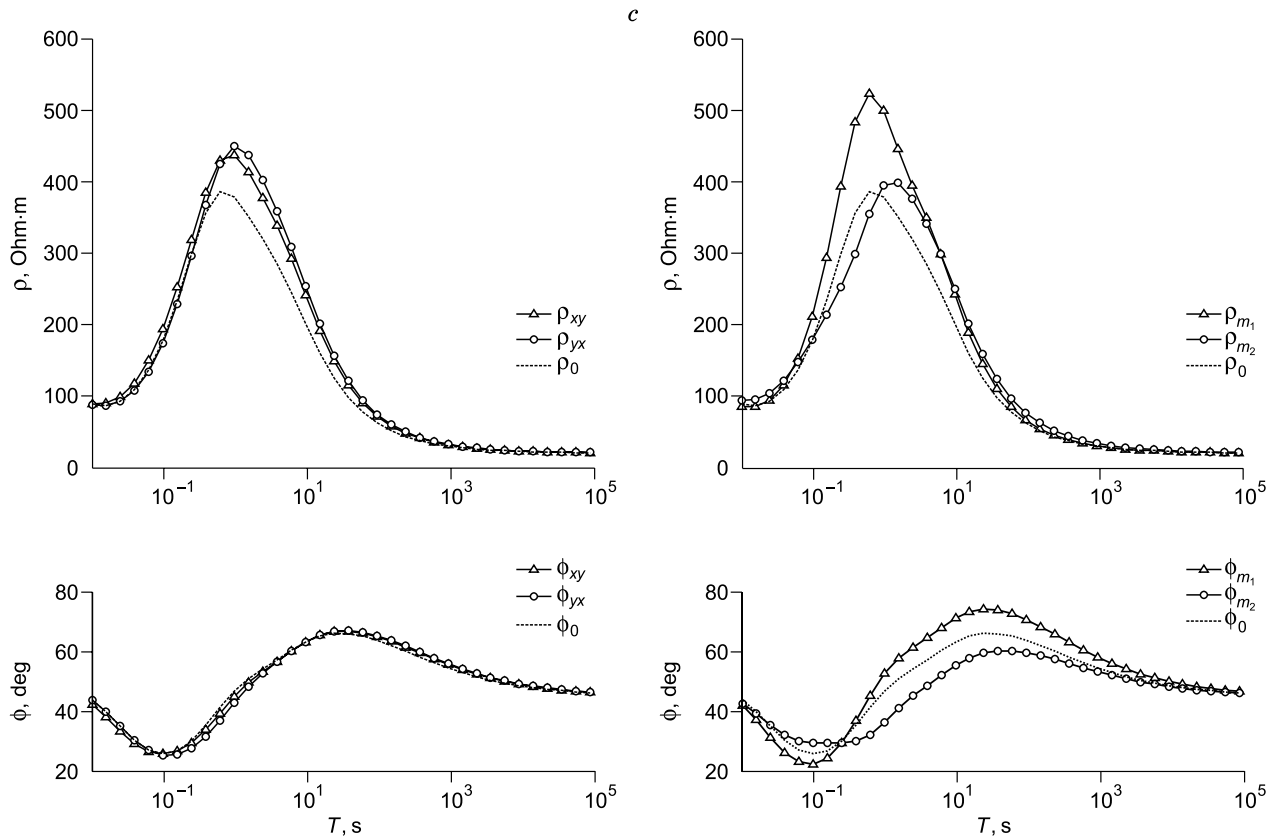


Fig. 1 (continued).

tween the magnetic field and the vertical direction was $\vartheta = 25^\circ$.

Figure 2 shows the results of calculation of MTS curves at the central station of the test site for an earth model with lateral heterogeneity. On time periods of more than 10 s, the MTS curves have distortions—the same static shift of the amplitude curves of ρ_{xy} and ρ_{yx} relative to the local curve of ρ_0 at the sounding station (by the local curve is meant the curve for a horizontally layered earth with the electrical conductivity dependent on depth at this station). In the case where the Hall effect is absent (Fig. 2a), the mode curves coincide with each other and with the standard curves (due to the symmetry of the lateral heterogeneity for the station under consideration, the additional impedances Z_{xx} and Z_{yy} are zero). However, with the occurrence of low Hall conductivity (Fig. 2b), the difference of the mode curves for the normal waves becomes already noticeable.

Consider now the polar diagrams in Fig. 3 for the standard impedances at the station under consideration. The diagrams for the principal impedances Z_{xy} almost correspond to a horizontally layered earth. The same is true for the diagram for the additional impedance Z_{xx} for $\sigma_H = 0$ (Fig. 3a). Considering the Hall conductivity (Fig. 3b), the diagram for Z_{xx} becomes similar to that for the case of two-dimensional heterogeneity, and the direction of the axes of symmetry also depends on the σ_H .

Thus, at the station above the center of the lateral heterogeneity studied, we can detect the influence of the Hall effect and estimate σ_H by analyzing the relation of the mode curves and considering the shape of the polar diagram for the additional impedance.

However, at other stations outside the lateral heterogeneity, where Z_{xx} and Z_{yy} are not zero even for $\sigma_H = 0$, they make their formal contribution to the mode impedances in accordance with (11). At these stations, it is difficult to detect the influence of the Hall effect from the mode curves and the additional impedance polar diagram.

There is another opportunity to detect the Hall effect in the case of symmetric lateral heterogeneity. As shown by the calculations, at the stations located directly on the OX or OY axes, the impedances Z_{xx} and Z_{yy} are zero only when $\sigma_H = 0$. Therefore, the mode curves at them coincide only in this case. Their difference is completely determined by the value of σ_H . This also makes possible its experimental evaluation. To obtain more reliable results, it is necessary to make estimates for two symmetrically located stations, since the picture in them must coincide.

An interesting result is obtained in the case of two-dimensional lateral heterogeneity. To study it, the resistivity of the upper layer in the latter earth model was assumed to vary linearly along the OX axis between values of 0.8 and 1.2 Ohm·m at the edges of the test site. Polar diagrams for

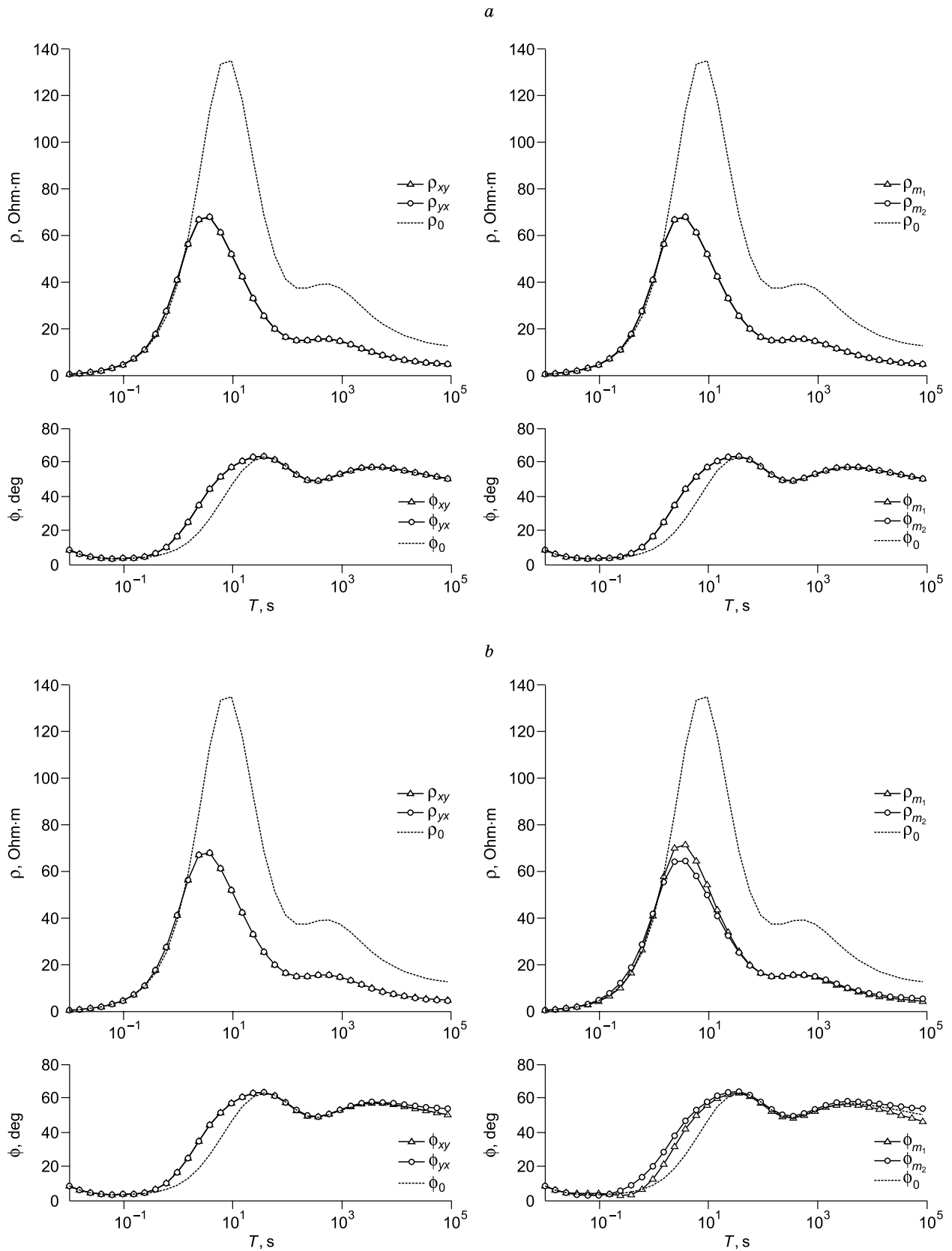


Fig. 2. MTS curves for the station above the center of the lateral surface heterogeneity (on the left are the standard curves, on the right are the mode curves, and the dotted lines show local curves). Here and in Figs. 3 and 4, the calculations were performed for $\sigma_H = 0$ (a) and $\sigma_H = 1/2000$ S/m (b).

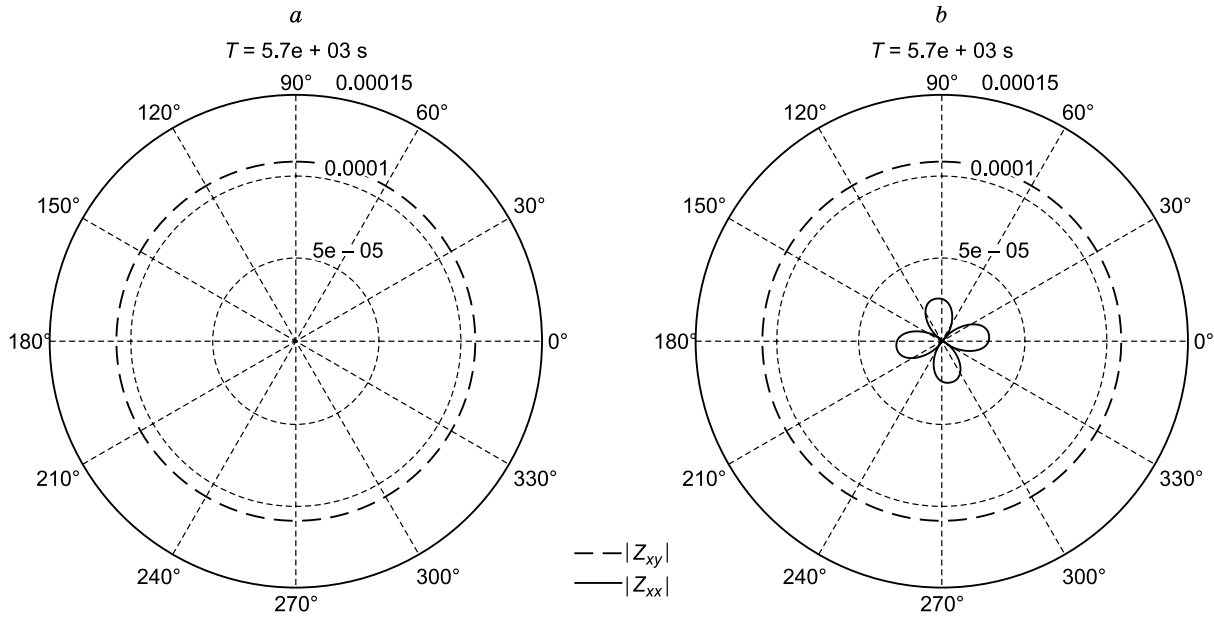


Fig. 3. Polar diagrams on a period $T = 5.7 \times 10^3$ s for the station above the center of the lateral surface heterogeneity (for clarity, the amplitude of the curve of $|Z_{xx}|$ is increased tenfold).

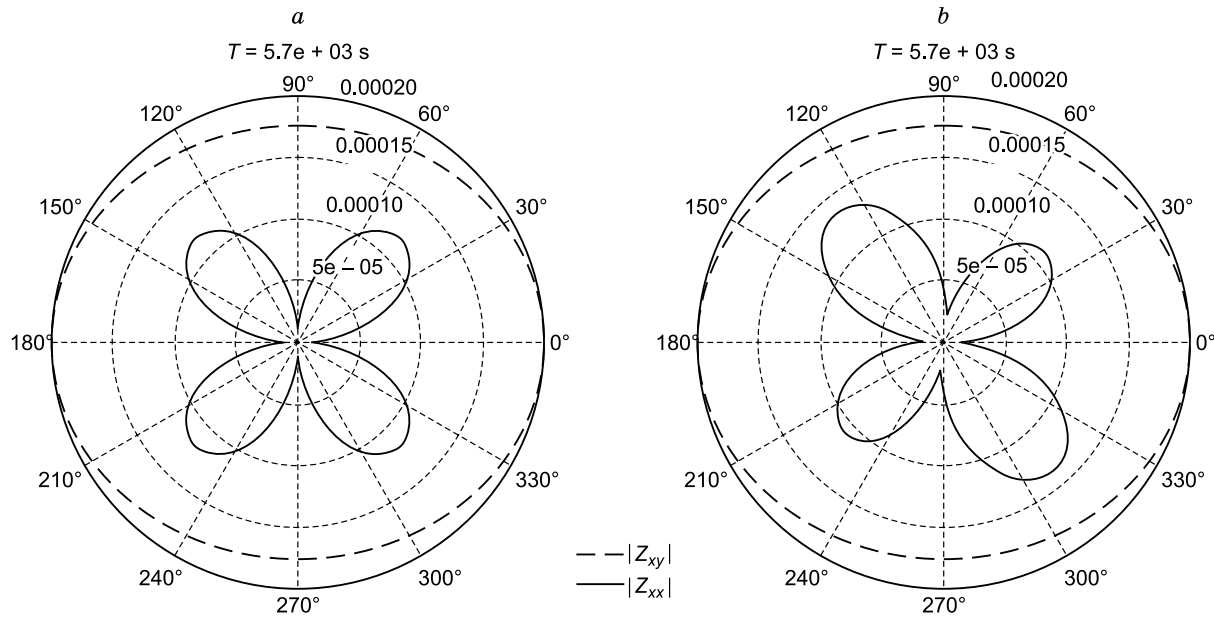


Fig. 4. Polar diagrams on a period $T = 5.7 \times 10^3$ s for the same station above the two-dimensional lateral surface heterogeneity (for clarity, the amplitude of the curve of $|Z_{xx}|$ is increased tenfold).

this case are shown in Fig. 4. It can be seen that the diagrams for the additional impedances with and without σ_H are noticeably different.

Some further explanation of the adopted value σ_H is in order. In the calculations, a Hall conductivity of 0.001 S/m was used only for the greater clarity of the figures and the description of the proposed technique. It is clear that with decreasing σ_H , it is more difficult to notice manifestations of the Hall effect. As an example, Fig. 5 shows the results of

calculations for a model with layers with top-to-bottom thicknesses of 0.005, 15, 10, and 45 km and resistivities of 10, 2000, 10, and 100 Ohm·m, respectively, and an underlying medium with a resistivity of 1 Ohm·m. The magnitude of the Hall conductivity was set two orders of magnitude lower, $\sigma_H = 0.00002$ S/m. The calculations were performed for the cases of the Hall conductivity present (1) in all layers of the model and (2) only in the uppermost thin layer. The results for both cases are practically identical in magnitude.

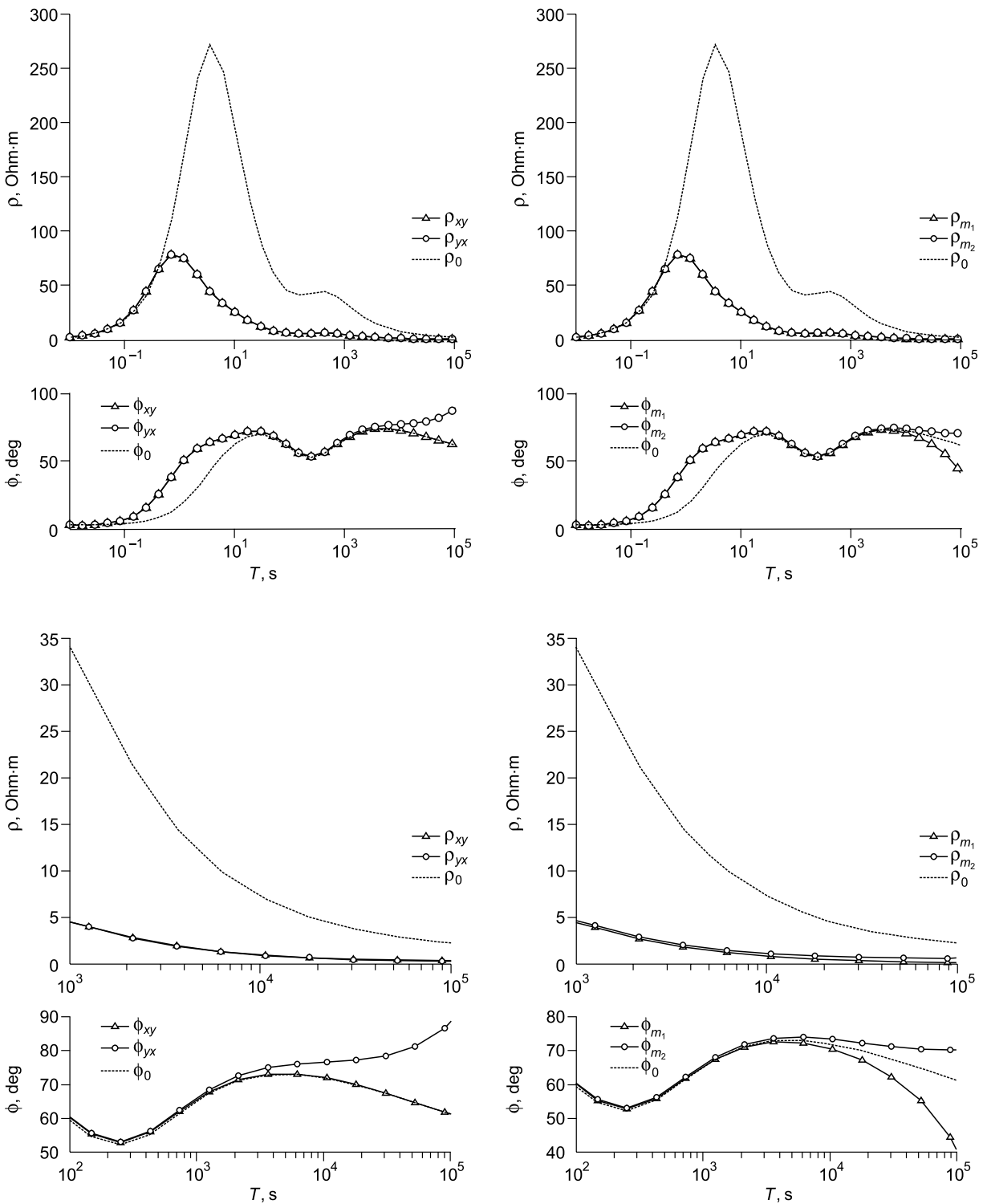


Fig. 5. MTS curves for the station above the center of the lateral surface heterogeneity (on the left are the standard curves, on the right are the mode curves, and the dotted lines show local curves, $\sigma_H = 0.00002$ S/m). At the top, the curves are shown for all periods, and at the bottom, with an enlargement for large periods.

This leads to the conclusion that for small values of the Hall conductivity, the contribution of deeper layers to the magnitude of the effect significantly decreases in this model. It is also seen that for $\sigma_H = 0.00002$ S/m, the manifestations of the effect are less pronounced: they are present only on periods longer than 10^3 s and more pronounced in the behavior of the impedance phases.

CONCLUSIONS

One of the experimental methods for determining the electrical conductivity of semiconducting minerals is based on the Hall effect. Considering the presence of the Earth's magnetic field, one can expect the Hall effect to manifest itself under the natural conditions of occurrence of these minerals when conducting electromagnetic soundings. Manifestations of the Hall effect were considered and numerical estimates of its magnitude were obtained which can be used to experimentally detect the Hall effect in magnetotelluric sounding.

Electrical conductivity was expressed in tensor form to take into account the effect of the Hall conductivity on measurement results. Since, in practice, there are lateral electrical conductivity heterogeneities, the calculations were carried out for a three-dimensional heterogeneous earth. For their implementation, the Trefftz method was chosen and its modifications suitable for an anisotropic earth were developed. In the numerical calculations, the anomalous field due to the earth anisotropy was determined. Numerical solutions for an isotropic three-dimensional heterogeneous earth were used as the normal field. The distortions of MTS curves due to near-surface lateral heterogeneities were taken into account. For different earth models, the standard impedance tensor was determined, which was converted to the mode impedances for the normal components of the anisotropic case.

Methods of accounting for the Hall effect were described, and its magnitudes that can be detected by modern electromagnetic sounding methods were numerically estimated.

It is found that manifestations of the Hall effect are the easiest to detect in the case of symmetric lateral heterogeneity. When the Hall effect is absent, the mode curves at the station located above the center of such heterogeneity coincide with each other. However, with the occurrence of low Hall conductivity, the difference of the mode curves for the normal waves becomes significant.

The influence of the Hall effect can also be detected by analyzing the shapes of additional impedance polar dia-

grams, including in the case of two-dimensional lateral heterogeneity.

In the calculations, a Hall conductivity of 0.001 S/m was only used for greater clarity of the figures and the description of the proposed method. Calculations have shown that the effect remains pronounced even at one or two orders of magnitude smaller values of the Hall conductivity. It cannot be ruled out that in practice this effect is even weaker. On the other hand, if everything were that simple, the Hall effect would have long been detected in both numerical and real experiments. Given the importance of earth parameters such as the mobility of current carriers and Hall conductivity, we would like this paper to draw greater attention of experts to this effect to perform specifically designed experiments.

We are grateful to the reviewers Yu.A. Dashevskii and L.A. Tabarovskii for their attention to this work and useful discussions.

This work was partially supported by the Russian Foundation for Basic Research (grant No. 17-05-00083).

REFERENCES

- Aleksandrov, P.N., 2001. The forward problem of geoelectrics in a one-dimensional bianisotropic medium. *Fizika Zemli* 37 (4), 51–61.
- Bush, G., 1952. Electronic Conductivity of Non-Metals. *Uspekhi Fizicheskikh Nauk* 47 (2), 258–324.
- Gololobov, D.V., Malevich, I.Yu., 2005. Physical and electrochemical processes in the medium above a hydrocarbon reservoir. *Dokl. BGUIR*, No. 1, 22–27.
- Egorov, I.V., 2011. Trefftz method for the solution of three-dimensional forward and inverse problems of geoelectrics. *Fizika Zemli* 47 (2), 15–26.
- Mogilatov, V.S., 2013. Influence of the geomagnetic field on the transient process of the secondary currents in Earth. *Geofizika*, No. 4, 70–75.
- Plotkin, V.V., 2017. Method for determining the contribution of the Hall effect in magnetotelluric sounding, in: XIII Int. Sci. Congress and Exhibition INTEREXPO GEO-SIBERIA-2017. Int. Sci. Conf. "Subsoil Use. Mining. New Directions and Technologies of Prospecting, Exploration and Development of Mineral Deposits. Geology" (electronic edition) [in Russian]. Novosibirsk, SGGa, Vol. 2, No. 3, pp. 187–192.
- Plotkin, V.V., Gubin, D.I., 2015. Accounting for near-surface heterogeneities over a horizontally layered section in magnetotelluric sounding. *Russian Geology and Geophysics (Geologiya i Geofizika)* 56 (7), 1083–1090 (1381–1390).
- Parkhomenko, E.I., 1967. *Electrical Properties of Rocks*. New York, Plenum Press.
- Shuey, R.T., 1975. *Semiconducting Ore Minerals*. New York, Elsevier Scientific Publishing Company.